

Document downloaded from:

<http://hdl.handle.net/10251/76456>

This paper must be cited as:

Pasquato, M.; Medici., C.; Friend, A.; Francés, F. (2015). Comparing two approaches for parsimonious vegetation modelling in semiarid regions using satellite data. *Ecohydrology*. 8(6):1024-1036. doi:10.1002/eco.1559.



The final publication is available at

<http://dx.doi.org/10.1002/eco.1559>

Copyright WILEY-BLACKWELL, 111 RIVER ST, HOBOKEN 07030-5774, NJ USA

Additional Information

Comparing two approaches for parsimonious vegetation modelling in semiarid regions using satellite data

Marta Pasquato¹, Chiara Medici^{1,3}, Andrew D. Friend² and Félix Francés¹

1: Research Institute of Water and Environmental Engineering, Universitat Politècnica de València, Spain.

2: Geography Department, University of Cambridge, UK.

3: Civil and Environmental Engineering; Princeton University; Princeton, NJ, USA.

Corresponding author: F. Francés, Research Institute of Water and Environmental Engineering, Universitat Politècnica de València, Camino de Vera s/n, Valencia, 46022, Spain (ffrances@upv.es).

Reference this paper as:

M. Pasquato, C. Medici, A.D. Wade and F. Francés (2015). Comparing two approaches for parsimonious vegetation modelling in semiarid regions using satellite data. *Ecohydrology*, 8, 1024-1036. DOI: 10.1002/eco.1559

Abstract

Large portions of Earth's terrestrial surface are arid or semiarid. As in these regions the hydrological cycle and the vegetation dynamics are tightly interconnected, a coupled modelling of these two systems is needed to fully reproduce the ecosystem behaviour and to predict possible responses to climate change. In this paper, the performance of two parsimonious dynamic vegetation models, suitable for the inclusion in operational ecohydrological models and based on well-established but different approaches, are compared in a semiarid Aleppo Pine region. The first model (WUE-model) links growth to transpiration through water use efficiency (WUE); the second model (LUE-model) simulates biomass increase in relation to absorbed photosynthetically active radiation (APAR) and light use efficiency (LUE). Furthermore, an analysis of the information contained in MODIS products is presented to indicate the best vegetation indices to be used as observational verification for the models. EVI is reported in literature to be highly correlated with leaf area index so it is compared with modelled LAI_{mod} ($r_{WUE-model}=0.45$; $r_{LUE-model}=0.57$). In contrast, NDVI appears highly linked to soil moisture, through the control exerted by this variable on chlorophyll production, and is therefore used to analyze LAI^*_{mod} , models' output corrected by plant water-stress ($r_{WUE-model}=0.62$; $r_{LUE-model}=0.59$). MODIS LAI and ET are found to be unrealistic in the studied area. The performance of both models in this semiarid region is found to be reasonable. However, the LUE-model presents the advantages of a better performance, the possibility to be used in a wider range of climates and to have been extensively tested in literature.

1 Introduction

A large portion of Earth is arid or semiarid (Renard *et al.*, 1993). These water-limited ecosystems are complex and their dynamics depend on multiple interconnections between climate, soil and vegetation (Rodriguez-Iturbe *et al.*, 2001). Projections of the IPCC (IPCC, 2007) indicate the high probability of an increase in the extent of drought-affected regions and a decrease in water resources in many semiarid areas. The potential adverse impacts on sectors

such as agriculture or water supply makes an in-depth knowledge of the dynamics of these environments vital (Cayrol *et al.*, 2000).

In the last few years there has been an increasing awareness of the critical role of vegetation in soil moisture dynamics (Scanlon *et al.*, 2005; Teuling and Troch, 2005; Ponce-Campos *et al.*, 2013) and groundwater resources (Le Maitre *et al.*, 1999; Scanlon *et al.*, 2006). For this reason, a great deal of effort has been made by ecohydrologists in modelling vegetation dynamics along with the hydrological cycle (Zalewski *et al.*, 1997; Hannah *et al.*, 2004). In order to be suitably coupled with operational hydrological models, vegetation models need to only require information commonly available in practical hydrological applications (Arora, 2002; Montaldo *et al.*, 2005).

Two different parsimonious approaches to hydrological-vegetation modelling in arid and semiarid environments can be found in literature. The first group of models simulates gross primary production (GPP) as a function of plant transpiration (T) through an ecosystem water use efficiency (WUE), which is the amount of carbon gained for unit of water loss (Williams and Albertson, 2005; Istanbuluoglu *et al.*, 2012). The second group of models simulates GPP as a function of intercepted light and light use efficiency (LUE), the ratio between the unstressed canopy carbon assimilation rate and the photosynthetically active radiation absorbed by the canopy (APAR) (e.g. Arora, 2002; Polley *et al.*, 2011). With the objective of identifying reliable ecohydrological models, and to explore new strategies to solve the problem of model validation, we present on the one hand a comparison between the described modelling approaches and on the other hand an analysis of collocated satellite data. Moderate-Resolution Imaging Spectroradiometer (MODIS) remote sensing products are evaluated in order to ascertain the value of the information that can be extracted from remote sensing data, and therefore determine how useful they may be as observational verification for the analysed models. This evaluation foreruns the model comparison and takes into account the fact that external conditions (e.g. soil moisture, soil colour) and the canopy structure can alter the computed vegetation indices values (Jackson and Huete, 1991). Satellite data information is contrasted with published observations regarding LAI reference values and seasonality in Mediterranean forests.

Therefore, in this paper we address the following questions. (1) Which of the two proposed parsimonious approaches to vegetation modelling performs best in a semiarid environment and hence should be recommended in a coupling process with an operational hydrological model? (2) Which satellite data sets are most suitable for characterizing vegetation dynamics in semiarid environments and could be used to assess the performance of the models?

2 Methods

2.1 Study area

The research site (centred in 37°46'N, 2°00'W) is a 20 km² Aleppo Pine (*P. halepensis* Mill.) open forest in the Valdeinfierno catchment, south east of Spain in the Andalusia region. Altitude is between 850 and 1350 m a.s.l.. The soil is a dolomitic lime. Rainfall occurs mostly in the autumn and spring and the average annual precipitation over the period 1933 – 2010 was 320 mm, having fluctuated between 99 mm and 884 mm. Mean monthly maximum air temperature ranges between 11°C (December and January) and 31°C (July and August), while mean monthly minimum temperature ranges between 1°C (from December to February) and 15°C (July and August). The mean annual reference evapotranspiration (ET_o) is 1130 mm (Hargreaves equation; Valdeinfierno meteorological station data: 1933 - 2010), much higher than annual mean precipitation, making water a strongly limiting resource. According to Köppen climatic classification, the climate is defined as semiarid.

2.2 Satellite Data

MODIS instruments flying onboard the Terra and Aqua satellites have been designed to provide valuable information on vegetation state at basin scale. Processed data are made openly available through online tools such as Reverb and GloVis. The satellite information used in this study is the following: the Normalized Difference Vegetation Index (NDVI) and the Enhanced Vegetation Index (EVI), both included in the products MOD13Q1 and MYD13Q1 (Huete *et al.*, 2002) and provided every 16 days at 250-meters spatial resolution; the Leaf Area Index (LAI), included in the products MOD15A2 and MYD15A2 (Myneni *et al.*, 2002) and provided every 8 days at 1000-meters spatial resolution; the

actual Evapotranspiration (ET), included in the MOD16A2 (Mu *et al.*, 2011) product and provided every 8 days at 1000-meters spatial resolution.

LAI is defined as the one sided green leaf area per unit ground area in broadleaf canopies, or as the projected leaf area per unit ground area in needle canopies.

NDVI and EVI are directly calculated from the reflectance registered by the satellite sensors in the Near-Infrared (NIR) (841-876nm), Red (620-670nm) and Blue (459-479nm) wavelengths as follows:

$$NDVI = \frac{(NIR - Red)}{(NIR + Red)} \quad (1)$$

$$EVI = G \cdot \frac{(NIR - Red)}{(NIR + C1 \cdot Red - C2 \cdot Blue + L)} \quad (2)$$

where L , $C1$, $C2$ and G are parameters that, in the MODIS-EVI algorithm, assume the values: 1; 6; 7.5; and 2.5 respectively. NDVI is sensitive to green leaf biomass (Tucker, 1979) while EVI has been found to be responsive to both LAI and canopy structure (Gao *et al.*, 2000). For these reasons, these two vegetation indices provide complementary information, extremely valuable when studying vegetation by means of remote sensing.

MOD15A2 and MYD15A2 LAI datasets are created by an algorithm that exploits the spectral information content of MODIS surface reflectances, requiring at the same time a land cover classification (Myneni *et al.*, 2003). This algorithm utilizes data from the MODIS Surface Reflectance Product (MODAGAGG) and the MODIS Land Cover Product (MOD12Q1).

As an alternative, LAI can be obtained from NDVI through an application of Beer's general equation as in *Lacaze et al.* (1996) and *Gigante et al.* (2009):

$$LAI_{NDVI} = -\frac{1}{k} \ln \frac{NDVI_{can} - NDVI}{NDVI_{can} - NDVI_{back}} \quad (3)$$

where $NDVI_{can}$ (canopy) is the value to which NDVI tends at high vegetation density, $NDVI_{back}$ (background) is the NDVI value corresponding to very low

vegetated soil and k is the extinction coefficient. $NDVI_{can}$ and $NDVI_{back}$ may be retrieved from the NDVI images (Anselmi *et al.*, 2004). The parameters used in this study were $NDVI_{can} = 0.9915$; $NDVI_{back} = 0.0549$ and $k = 0.212$ (Anselmi *et al.*, 2004).

The ET product contains data evaluated using Mu *et al.*'s algorithm (2011), which is based on the Penman-Monteith equation (Monteith, 1965). Land cover classification, albedo, LAI and FPAR information, necessary for the calculations, are obtained from the MODIS Land Cover Product (MOD12Q1), the MODIS Land Surface Albedo Product (MOD43B3) and the MODIS Leaf Area Index and Fractional Photosynthetically Active Radiation Product (MOD15A2) respectively.

2.3 Vegetation models

Two approaches to dynamic vegetation modelling are implemented here to evaluate their ability to simulate the evolution of carbon and water exchange processes in a semiarid region. Simulations are performed with a daily time step, on a per unit ground area basis. Equations are solved with finite difference approximations, using at each time step the variable values calculated at the previous one. The dynamics of vegetation biomass are in both cases modelled through a mass balance. In one case growth is based on transpiration (T) and takes into account the Water Use Efficiency (WUE) factor; in the other case carbon uptake is based on photosynthesis, simulated through the Absorbed Photosynthetically Active Radiation and the Light Use Efficiency (LUE) factor.

Both approaches consider respiration in order to estimate net primary production. Part of this total production is allocated to leaves, according to the maximum leaf biomass that can be sustained by the system. The modelled state variable is the leaf biomass (B_l , kg DM m⁻² vegetation cover; where DM denotes dry matter), from which leaf area index (LAI_{mod} , m² leaf m⁻² ground) can be calculated by means of the specific leaf area (SLA, m² leaf kg⁻¹ DM) and the fraction of vegetated area (f_t , m² vegetation cover m⁻² ground), providing the possibility to compare models results with satellite products. Turnover, caused by leaf ageing, is then taken into account.

Real structural LAI changes more slowly than remotely sensed NDVI, which reflects chlorophyll and leaf angle adjustments before loss of structural tissues and leaf drop. In fact, Mediterranean summer drought is reported to induce a

generalized decrease in chlorophyll, as a mechanism of protection (Kyparissis *et al.*, 1995). In particular, Aleppo Pine showed a 25% reduction in chlorophyll content when a 30 month water stress treatment was applied and soil water potential was maintained at -400 kPa (Baquedano and Castillo, 2006). For this reason, to compare model results with LAI_{NDVI}, it is advisable to scale LAI_{mod} by vegetation water stress (see Appendix A), as in Sellers *et al.* (1996) and Williams and Albertson (2005), obtaining in this way LAI*_{mod} (m² green leaf m⁻² ground). Considering the properties of the model outputs and of the available satellite indices, it appears suitable to compare LAI*_{mod} with LAI_{NDVI} and also LAI_{mod} with EVI, the latter being very responsive to structural LAI.

Soil moisture in the effective root zone is the result of the balance between incoming precipitation (P) and leaf interception (I) and the losses produced by evaporation from bare soil (E), transpiration (T) and leakage (L). The effective soil depth is divided into two layers: a shallow layer that is implicated in the processes of bare soil evaporation and superficial roots' transpiration, and a second underlying layer that provides soil moisture to deeper roots. Actual evapotranspiration (see Appendix B) is based on reference values, corrected by a water stress function. Models are forced by daily inputs of precipitation, air temperature and radiation.

2.3.1 Carbon balance for WUE-model

Similar to Williams and Albertson (2005) the leaf biomass dynamics are modelled as:

$$\frac{dB_l}{dt} = (T \cdot WUE \cdot \rho_v \cdot \omega - Re) \cdot \varphi_l - k_l \cdot B_l \quad (4)$$

where B_l is the leaf biomass (kg DM m⁻² vegetation cover). φ_l is fractional leaf allocation, k_l is leaf natural turnover factor, and Re is respiration, each described with more details in Appendix A. ρ_v and ω are the density of water (Mg m⁻³) and the conversion of CO₂ exchange to dry matter (kg DM kg⁻¹ CO₂), needed to convert the units. WUE is calculated with air diffusivities of CO₂ and

H₂O vapour, ambient CO₂ concentration and saturated specific air humidity dependence, as in Williams and Albertson (2005).

This model is built on the hypothesis that water is the limiting factor for vegetative growth: the assumption made is that the control exerted over transpiration by soil moisture can be shifted to growth, so that it results in growth itself being controlled only by water availability. Consequently, the very basis of this model makes it appropriate only for simulations in arid and semiarid climate, excluding any environment where factors, other than water availability, control vegetation development.

2.3.2 Carbon balance for LUE-model

It has been hypothesized (Monteith, 1972; Monteith and Moss, 1977; Jarvis *et al.*, 1983) that there should be a strong positive relationship between plant biomass production by terrestrial vegetation and absorbed photosynthetically active radiation in ideal conditions. The proportionality between dry matter production and light absorption is known as light use efficiency (LUE), and this relationship has been widely used in vegetation modelling (e.g. Knorr and Heimann, 1995; Ruimy *et al.*, 1999; Running *et al.*, 2000; Running *et al.*, 2004; Montaldo *et al.*, 2005). Stress conditions, such as water or nutrient deficit, tend to diminish LUE value (Green *et al.*, 1985; Li *et al.*, 2008) so that a correction factor has to be applied in these situations.

The second tested model simulated the leaf biomass (B_l , kg DM m⁻² ground) as follows:

$$\frac{dB_l}{dt} = (LUE \cdot \varepsilon \cdot PAR \cdot FPAR - Re) \cdot \varphi_l - \kappa_l \cdot B_l \quad (5)$$

where ε takes into account the reduction in LUE due to stress sources. In this study, because of the semiarid climate, the water deficit was considered dominant over other causes of stress; hence ε is calculated as $(1-\zeta)$, where ζ is water stress. Monthly averaged photosynthetically active radiation (PAR) was obtained from the incident global radiation provided by the World Radiation Data Centre, using a constant ratio of 0.48 MJ (PAR) MJ⁻¹ (global radiation)

(McCree, 1972). The total fraction of incident PAR absorbed by the canopy (FPAR) was estimated with the Beer's law:

$$FPAR = 0.95 \cdot (1 - \exp(-k \cdot LAI_{\text{mod}})) \quad (6)$$

where k is the light extinction coefficient over canopy. LAI_{mod} is the value of LAI as simulated by the model. Details are given in Appendix A. As in the WUE-model, R_e , ϕ_l and k_l are respiration, fractional leaf allocation and leaf natural decay factor respectively, and are described in Appendix A.

Table 1. Range of parameters values considered for calibration and sensitivity analysis.

| Parameter | Description | Minimum bound | Maximum bound | Sources ^a |
|--------------------|--|---------------|---------------|----------------------|
| LAI_{max} | Maximum LAI [m^2 leaf m^{-2} vegetation] | 1 | 2 | 1, 2 |
| SLA | Specific leaf area [m^2 leaf kg^{-1} DM] | 1.5 | 2.5 | 3 |
| ω | Conversion of CO_2 to DM [kg DM kg^{-1} CO_2] | 0.4 | 0.7 | 4 |
| LUE | Light use efficiency [$\text{kg C m}^{-2} \text{MJ}^{-1}$] | 1.8 | 2.2 | 5 |
| I_{max} | Maximum interception [mm d^{-1}] | 0.5 | 5 | 6 |
| r_1 | Fraction of roots in upper soil layer [-] | 0.1 | 0.4 | 7 |
| d_1 | Thickness of first soil layer [mm] | 30 | 100 | 7 |
| d_2 | Thickness of second soil layer [mm] | 500 | 1100 | 7 |
| f_t | Vegetation fractional cover | 0.7 | 1 | 7 |

^a Sources: 1. Ceballos and Ruiz de la Torre (1979); 2. López-Serrano et al. (2000); 3. Awada et al. (2003); 4. De las Heras et al. (2013); 5. Yuan et al. (2007); 6. Crockford and Richardson (1990); 7. field campaigns.

2.4 Sensitivity analysis

To obtain an insight into the models' functioning and to assess which parameters mostly affect their performances, a general sensitivity analysis (GSA) (Hornberger and Spear, 1980) was performed on the two models. Eight parameters for each model were taken into account for the sensitivity analysis (Table 1). The parameters were selected because either specific of the plant species and the study site or difficult to be estimated from literature. The GSA

was based on the Monte Carlo technique; parameters values were randomly sampled from uniform distributions within ranges based on literature estimations or field observations, as specified in Table 1. 60,000 independent sets of parameters were generated; for each of them, LAI_{mod}^* time-series were simulated and the objective function Root Mean Square Error (RMSE) calculated, contrasting model outputs with LAI_{NDVI} (See section 3.1).

A threshold, identified by an RMSE value of 0.2, divided the parameters values sets into two groups: behavioural parameters, which led to satisfactory simulations (with a RMSE equal or less than the adopted threshold), and non-behavioural ones, that produced non-acceptable results (RMSE above the adopted threshold). A threshold of 0.2 was chosen because it was considered a reasonable RMSE, taking into account the models' potential performance. In addition, as the objective was the comparison between the two models, the choice of the same reasonable value for both models reduced the importance of the value itself. The analysis resulted in 3958 behavioural and 56042 non-behavioural simulations for the WUE-model, 16893 behavioural and 43107 non-behavioural simulations for the LUE-model. As in Medici et al. (2012), the cumulative probability distributions of the two groups were obtained and the Kolmogorov-Smirnov two-sample test (KS) was used to evaluate the relative importance of each parameter's contribution to the model simulation (Wade *et al.*, 2001). The KS index test statistic is equivalent to the maximum vertical distance between the cumulative probability distributions for the behaviours and non-behaviours. The larger the value of the KS index, the greater the importance of the considered parameter in determining the simulation result. The sensitivity analysis found that the parameter that most influences the WUE-model's outputs is LAI_{max} (KS index = 0.44), followed by I_{max} (KS = 0.31) and f_t (KS = 0.28). In the case of the LUE-model, the most influential parameter is d_1 (KS = 0.23), followed by LAI_{max} (KS = 0.2) and d_2 (KS = 0.12).

To test the models' robustness and their capability in reproducing the satellite-derived vegetation dynamics, a General Likelihood Uncertainty Estimation (GLUE) (Beven and Binley, 1992) was performed, taking into account only the behavioural sets of parameters. In this way, it was possible to calculate the likelihood-weighted distribution of the outputs corresponding to the accepted sets of parameters, and to compute the 5% and 95% GLUE bands. The GLUE

bounds are depicted in Figure 1. As far as the percentage of LAI_{NDVI} data included within the GLUE bands, 63% of the “observed” data were included within the WUE-model GLUE bounds, while 53% of them lie between the LUE-model bounds. Both models showed their lowest performances during autumn 2005 and from autumn 2007 to spring 2008 (Figure 1). In the first case, the recovery of LAI^*_{mod} after the summer minimum was too slow compared to LAI_{NDVI} evolution; in the second case, there was a much stronger decline in LAI^*_{mod} values with respect to LAI_{NDVI} ones, starting in November and till April. The GSA and GLUE analyses provide the possibility of understanding the simulation capability of the models. In this case, they reveal similar behaviours of the two models and a general accordance with satellite NDVI information. Analysing the two periods of poorest accordance between simulated LAI^*_{mod} of both models and LAI_{NDVI} , they appear clearly linked with the drought periods. The low precipitation periods in the study region (Figure 2) are reflected in the satellite data as well, but the effect is not as marked as in the models’ simulations.

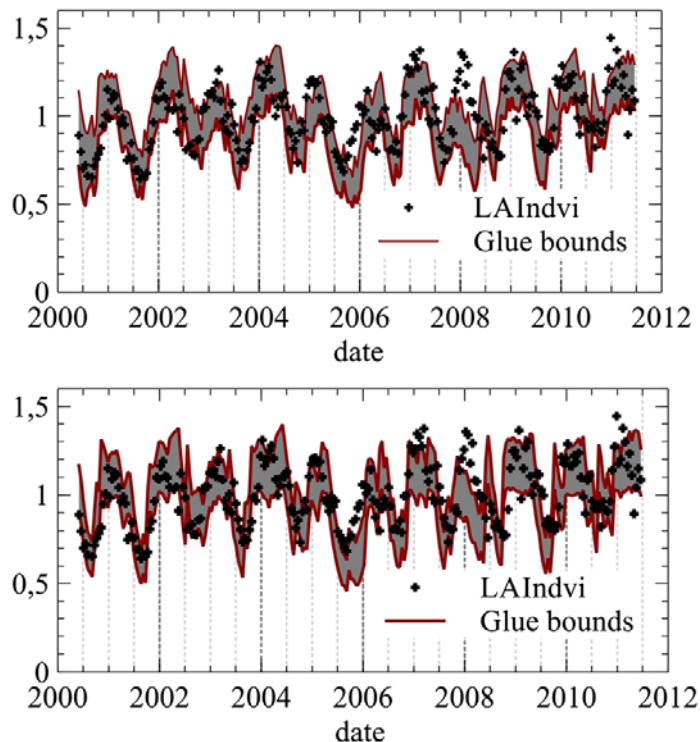


Figure 1. LAI_{NDVI} , as calculated from the satellite-recorded NDVI, with the 90% GLUE bands for the WUE-model (A) and the LUE-model (B).

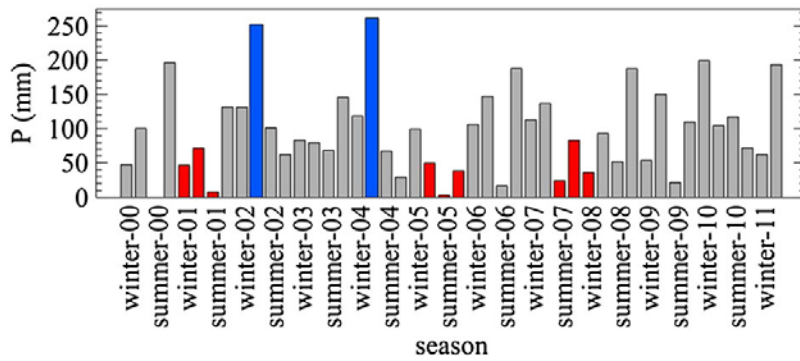


Figure 2. Seasonal precipitation (mm). Prolonged periods of low precipitation are shown in red, while the rainiest seasons of the studied period are shown in blue.

3 Results and discussion

3.1 Satellite data evaluation

Satellite EVI, NDVI, LAI and ET were analysed for the period 2000 – 2011 over the study area, averaging the spatial distributed data (320 cells in case of 250 m data spatial resolution, 80 cells in case of 500 m resolution) to obtain the evolution through time. A partial analysis of single cells was also performed, obtaining patterns that were similar to those of averaged datasets. This averaging process was nonetheless needed because at this stage the vegetation models, which refer to the satellite data as observational verification, work at an aggregate level.

All four products showed a marked seasonal quasi-sinusoidal behaviour, but differences between them, and particularly involving the NDVI, were noticed regarding the timing of peaks. This is perhaps surprising, as leaf area and NDVI would be expected to be correlated.

EVI peaks in April – May, followed by a decline until late autumn (Figure 3A). The peak of the index corresponds to the spring sprouting typical of Aleppo Pine in the Spanish area (Weinstein, 1989; Pardos *et al.*, 2003), and the drop is likely related to the summer shedding of needles accumulated in the previous 1 - 3 years (García-Plé *et al.*, 1995; Borghetti *et al.*, 1998; Calatayud *et al.*, 2000; Muñoz *et al.*, 2003). This suggests that EVI is responding to variations in LAI, as have been reported elsewhere (Gao *et al.*, 2000; Huete *et al.*, 2002).

With respect to the observations of NDVI, this index is sensitive to the “greenness” of the target and reaches its annual maximum between November and February (Figure 3A), when plants have completely recovered from the summer drought and leaf chlorophyll content is high (Kyparissis *et al.*, 1995; Baquedano and Castillo, 2006). Therefore, comparing EVI and NDVI series, it could appear that NDVI is shifted with respect to EVI. As a matter of fact, a second peak of NDVI occurs, presumably due to spring sprouting, and is correlated with EVI maximum. Hence NDVI is sensitive to different phenomena, recovery of pre-drought photosynthetic pigments level and growth of new shoots, with two distinct peaks. Similar contrasts between NDVI and EVI were found by Evrendilek and Gulbeyaz (2008) in Mediterranean forests in Turkey, although in that case, probably due to lower time resolution, NDVI double peaks were not identified, while just an apparent shift between the two indices was underlined.

The scatter plot of NDVI and EVI (Figure 3B) indicates a low general correlation between these datasets. A t-test was performed, and the presence of a significant correlation between NDVI and EVI series rejected at the 5% level. However, when dividing the data sets into two groups, one referring to months from October to March, and the other referring to months from April to September, still no correlation was found between the two indices for the former data group, while a significant positive correlation ($r = 0.66$) was highlighted for the latter group of data, suggesting that in this period the two indices are influenced by the same phenomenon (i.e. spring sprouting and summer shedding).

As far as the MOD15A2 product is concerned, the values of LAI provided, ranging between 0.2 and 0.8 (Figure 4), appear to be very low compared to values reported in literature (Sabaté *et al.*, 2002; Sprintsin *et al.*, 2007; Vicente-Serrano *et al.*, 2010; Molina and del Campo, 2012) for the same species in similar climatic conditions. Molina and Del Campo (2012), for example, report values of LAI = 0.5 and forest cover = 16% for high-intensity thinning treatment in Aleppo Pine forests. The vegetation in the study area is not as sparse as to justify similar LAI values. A likely explanation was found on analysing the data, where we found that the land cover classification, on which the algorithm used to compute LAI is based, does not correspond to the actual vegetation. The

area is classified partly as shrublands and partly as savanna. A similar problem was detected by Sprintsin et al. (2009) for the Yatir Aleppo Pine forest located in an arid-semiarid climatic area. For these reasons it was decided to reject the MOD15A2 data and refer only to EVI and NDVI for the estimation of vegetation biomass. Nevertheless, the timing of maxima and minima of satellite-derived LAI, which corresponds to EVI's one, appears to be correct considering the forest phenological cycle.

The product MOD16A2 provides an estimation of actual ET, ranging between 0.1 and 1.8 mm/d, and is statistically correlated with daily reference evapotranspiration (ET_o), with a Pearson coefficient $r = 0.79$. However, this high correlation is suspect, considering the semiarid climate that determines water stress, and therefore a decrease in transpiration rates, during the periods of highest ET_o . Considering that the MOD16A2 product that provides ET assessment is derived using MOD15A2 LAI product, and having rejected the MOD15A2 data, MOD16A2 is also considered potentially unreliable.

Having rejected the MOD15A2 product for the study area, it was necessary to rely on LAI_{NDVI} , which was calculated from NDVI through the Beer's law-derived approach. The apparent dependence of NDVI on leaf water content for Mediterranean forest is transferred to the derived index, making necessary a correction to the model's results by water stress as described in Appendix A, to allow comparison with LAI_{NDVI} . The calculated LAI_{NDVI} differed from MOD15A2 LAI product in timing (as between MODIS NDVI and LAI data) and in the range of variation, being LAI_{NDVI} higher in values and varying between 0.7 and 1.5 (Figure 4A). The scatter plot (Figure 4B) suggests the presence of two distinct groups of pairs of data. The total Pearson correlation coefficient is negative and statistically significant ($r = -0.37$). When dividing, as for NDVI and EVI, the datasets into two groups (April to September and October to March) the correlations result 0.63 and -0.29 respectively.

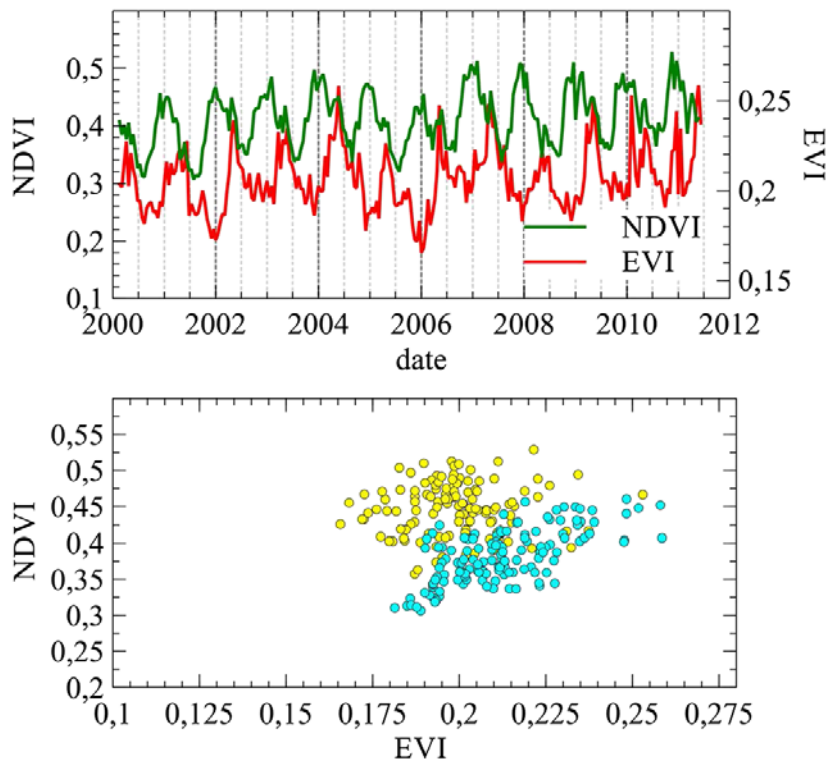


Figure 3. Comparison between EVI and NDVI, as obtained from satellite data: evolution in time (A) and scatter plot (B). In cyan blue, data referring to the months April to September; in yellow, data referring to the months October to March.

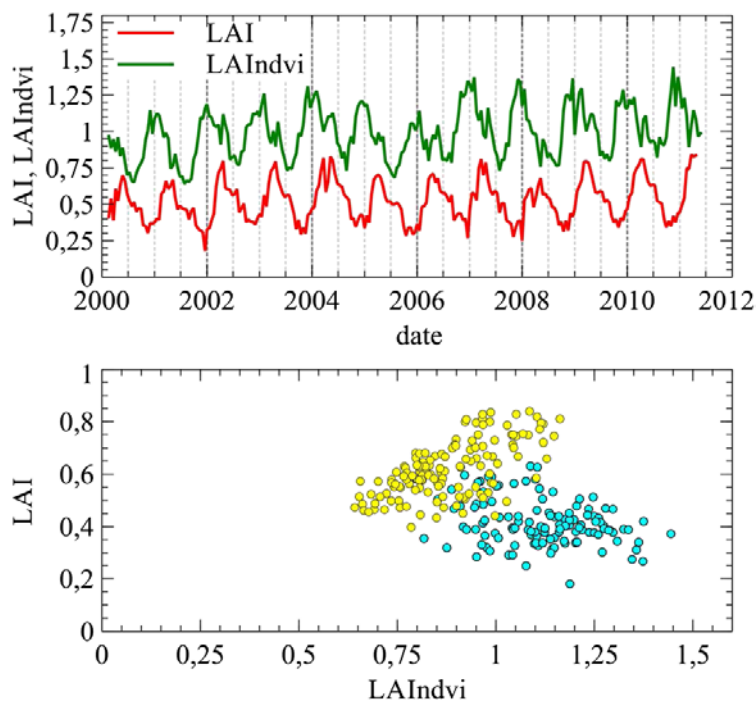


Figure 4. Evolution in time of LAI (MODIS MOD15A2 product) and LAI_{NDVI} obtained from NDVI data (A) and scatter plot of the two variables (B). In cyan

blue, data referring to the months April to September; in yellow, data referring to the months October to March.

3.2 Models evaluation

After evaluating the models' sensitivity, the same 8 parameters analysed in the sensitivity analysis were calibrated for each model, using the satellite information. A genetic algorithm was used to minimize the relative RMSE between the simulated LAI^*_{mod} and the LAI_{NDVI} .

A 4 months spin-up period was used, after which the system was found to be independent from the initial conditions. The simulations were finally run for the period June 2000 – June 2011, as satellite data were available for the same timespan. The final values assigned to parameters and constants, in order to run the simulations, are reported in Table 2.

The application of the two dynamic vegetation models gave the results in Figure 5 to Figure 8. Pearson correlation coefficients (r) between LAI_{mod} and EVI series were 0.45 for the WUE-model (Figure 5) and 0.57 for the LUE-model (Figure 7). When comparing LAI^*_{mod} and LAI_{NDVI} , r resulted in 0.61 and 0.60 for the WUE-model and the LUE-model respectively (Figure 6 and Figure 8), while the RMSE was 0.181 in the first case and 0.162 in the second one. Two tailed t-distribution statistical tests were performed to test the existence of statistically significant correlations between the considered variables (i.e.: LAI_{mod} vs. EVI and LAI^*_{mod} vs. LAI_{NDVI} , for both WUE-model and LUE-model). All correlations were highly significant, with $p < 0.0001$. Figure 9 shows the 11-year average of monthly LAI^*_{mod} and LAI_{NDVI} : seasonality is reasonably reproduced by both models, with LUE-model performing on average better.

After the calibration, the models presented the same qualities and problems indicated by the sensitivity analysis. In addition, for the WUE-model two further periods of discrepancy were found: winter-spring 2002 and spring 2004. The high precipitation rates (Figure 2), in conjunction with high reference evapotranspiration, resulted in elevated simulated plant transpiration. Considering that the WUE-model assumes a direct dependence of biomass production on transpiration, the simulated LAI^*_{mod} exceeds satellite-derived LAI_{NDVI} .

As a whole, the LUE-model performed best, with the lowest RMSE and the best agreement with averaged LAI_{NDVI} at monthly timescales for both amplitude and phase (Figure 9). This result is maybe unexpected, considering the fact that WUE-model has been specifically developed to be applied to arid and semiarid systems, and LUE should not be the driver of LAI in such environments. The better performance of the LUE-model might be explained by the fact that in this model the seasonal solar cycle reflected in PAR induces a seasonality on vegetation growth, concurring with the phenology of plant leaf onset. It is possible that this seasonality, modulated by water stress through the coefficient ϵ , is the driver of the good results and not much the fact that light availability is directly controlling plant growth. WUE-model has a less clear component of seasonality and tends to emphasize periods of water stress and above average water availability, which leads to a lower performance.

In addition to the better performance showed in this paper in semiarid environments the LUE-model has the capability to simulate vegetation dynamics in a wide range of environments (Medlyn, 1998), and the potential to take into account different types of stresses through a change in the formulation of ϵ , the LUE correction factor. Finally, it has been extensively used and evaluated in literature. For these reasons, it is probably the best choice when looking for a parsimonious vegetation model to be coupled to a conceptual hydrological model.

Although considered potentially unreliable because based on rejected MODIS LAI products, ET data provided by NASA were contrasted with the model simulations, to have the chance to better discuss the model results. The two sets of data presented the same seasonality, but two main differences could be identified: while satellite data did not show marked inter-annual variability in the peak values, both models presented significant differences between years, with the highest annual maximum value in 2002 and the lowest annual maximum value in 2005. In addition, simulations exhibited a relevant fall in ET values in August, when water stress reached its maximum values, while data processed from satellite information showed minor or no decline in the same period. These drops in the simulated ET values are sensible, considering the behaviour of plants at high levels of water stress, reinforcing the suspect of unreliability that lies on MOD16A2 data.

Table 2. Model Parameters and Constants.

| Parameters and constants | Description | Values | Sources ^a |
|-----------------------------|--|--------------|----------------------|
| LAI_{max} | Maximum LAI [m^2 leaf m^{-2} vegetation] | 1.4 | calib. |
| k_l | Leaf natural decay factor [d^{-1}] | 0.00137 | 1, 2 |
| SLA | Specific leaf area [m^2 leaf kg^{-1} DM] | 1.6 | calib. |
| I_{max} | Maximum interception [$mm d^{-1}$] | 1 | calib. |
| $\theta_{lim}, \theta_{cr}$ | Limit (lim), critical (cr) soil moisture [$m^3 H_2O m^{-3}$ soil] | 0.109, 0.256 | calc.(3) |
| r_1 | Fraction of roots in upper soil layer [-] | 0.1 | calib. |
| d_1, d_2 | Thickness of soil layers [mm] | 50, 950 | calib. |
| Ψ_{ae} | Air entry matric potential for loam [MPa] | 1.43E-03 | 3 |
| Ψ_{lim}, Ψ_{cr} | Matric potential at limit (lim), critical (cr) points [MPa] | 3, 0.03 | 4 |
| n | Porosity [m^3 void m^{-3} soil] | 0.451 | 3 |
| b | Soil parameter for loam [-] | 5.39 | 3 |
| ω | Conversion of CO_2 to DM [$kg DM kg^{-1} CO_2$] | 0.54 | calib. |
| ρ_v | Density of water [$kg m^{-3}$] | 10^3 | - |
| LUE | Light use efficiency [$kg C m^{-2} MJ^{-1}$] | 2.1 | calib. |
| f_t | Vegetation fractional cover | 0.89 | calib. |

^aSources: 1. Ceballos and Ruiz de la Torre (1979); 2. Calatayud et al. (2000); 3. Clapp and Hornberger (1978); 4. Laio et al. (2001).

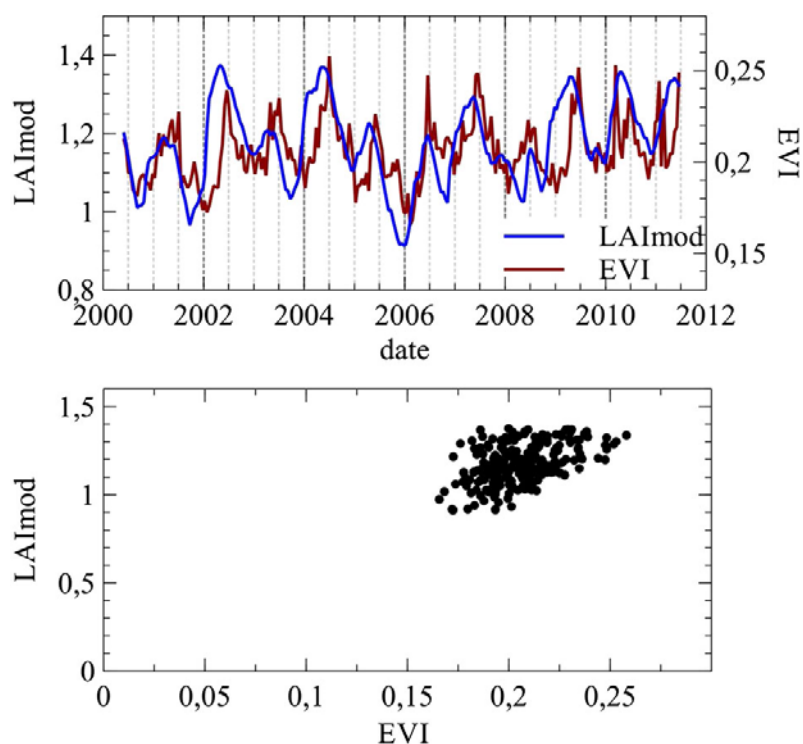


Figure 5. Results of the WUE-model where $LAI_{mod} = B_l \cdot SLA \cdot f_t$. Evolution in time and scatterplot.

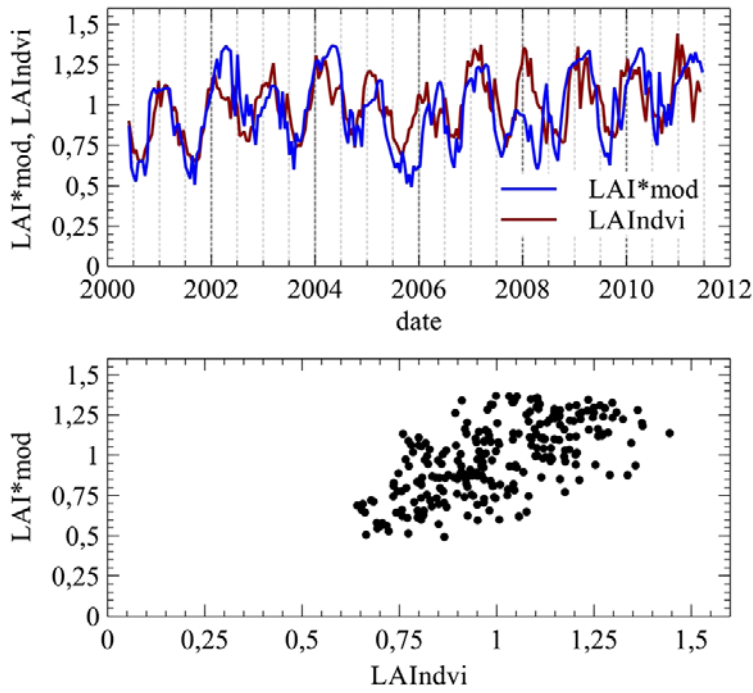


Figure 6. Results of the WUE-model, where LAI^*_{mod} is LAI_{mod} corrected by water stress; LAI_{NDVI} is the LAI obtained from NDVI as in Gigante et al. (2009). Evolution in time and scatterplot.

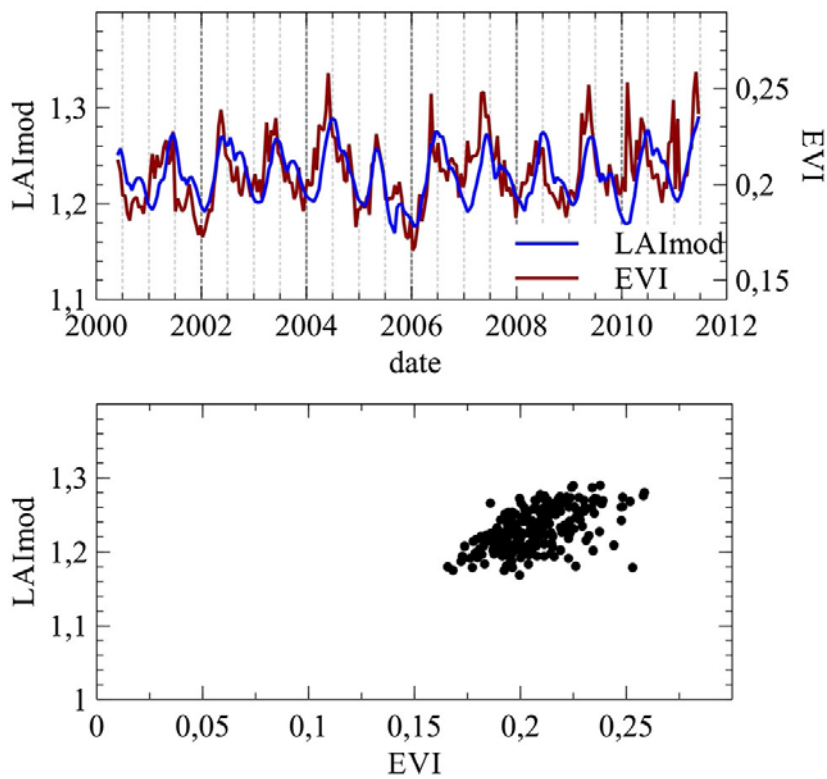


Figure 7. Results of the LUE-model, where $LAI_{mod} = B_l \cdot SLA \cdot f_t$. Evolution in time and scatterplot.

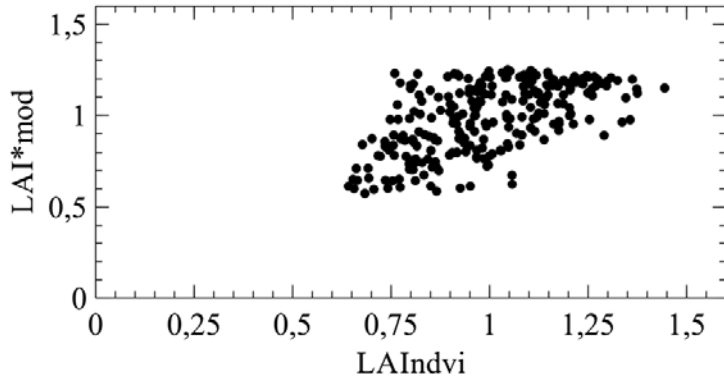
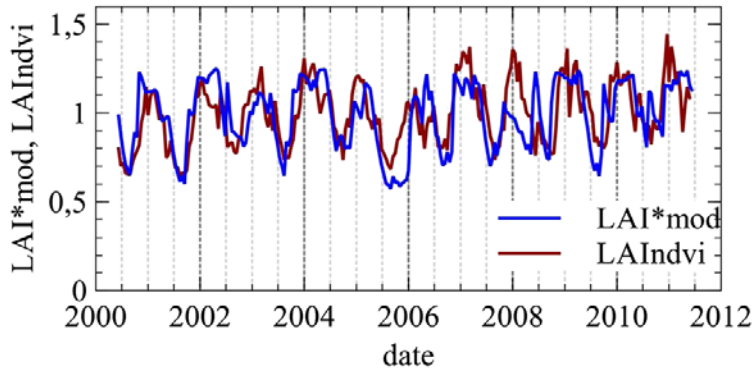


Figure 8. Results of the LUE-model, where LAI^*_{mod} is LAI_{mod} corrected by water stress; LAI_{NDVI} is the LAI obtained from NDVI as in Gigante et al. (2009). Evolution in time and scatterplot.

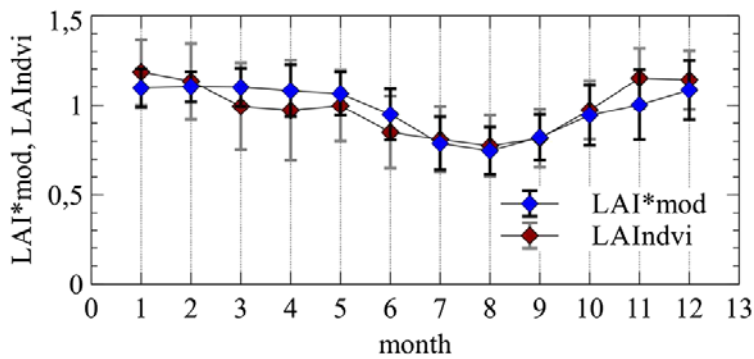
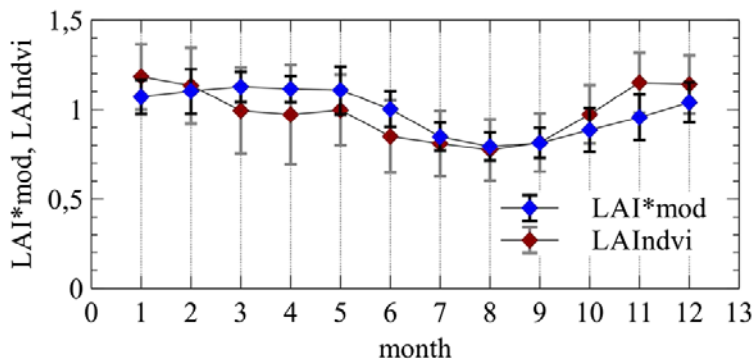


Figure 9. Satellite-derived LAI_{NDVI} and modelled LAI^*_{mod} averaged for each month of the year for the period 2000 to 2011, with bars indicating ± 1 standard deviation, for the WUE-model (A) and for the LUE-model (B).

4 Conclusions

Vegetation-related satellite products for a semiarid region of Spain were analysed in order to assess their relation with vegetation state and development. NDVI showed a strong dependence on soil moisture and leaf water content, explainable by the impact of water-stress on chlorophyll content in Aleppo Pine leaves. The EVI proved to be strongly related to biomass dynamics and to LAI in particular. As for the LAI values provided by LP DAAC, they are too low relative to published ranges for the same species in similar climatic conditions. A possible explanation for this difference was found in the wrong land cover classification used by the algorithm that provides an estimation of this index, based on satellite data. An in-depth analysis of satellite information prior to its use appears therefore crucial because, while well performing at a global scale, at a regional or local extent it may present important issues.

Once assessed the reliability of remote sensing EVI and NDVI, two parsimonious vegetation models, namely the WUE-model and the LUE-model, were tested in order to evaluate their capacities to reproduce the information gathered from the satellite vegetation indices. The two approaches proved capable of simulating the vegetation dynamics and performed similarly, with the LUE-model achieving slightly better results, particularly during the periods of concurrent high available soil moisture and high ET_0 . In these cases the WUE-model, linking growth to transpiration, overestimates biomass. Furthermore, considering that the WUE-model is specific for water limited environments only, while the LUE-model can be adapted to other types of ecosystems, the use of the latter is recommended when seeking a broadly applicable, simple vegetation model to be coupled with a conceptual hydrological model. Nonetheless, the WUE-model may be considered a valid option when dealing with water-limited systems, provided that the limits of this model, identified in the present study, are taken into account.

The research presented helps identifying the correct strategy to use remotely sensed data on Mediterranean ecosystems for model validation purposes, highlighting possible problems in some remotely sensed products that are commonly used in ecohydrological applications. Moreover, the performed simulations allow to identify the level of reliability of the vegetation models selected.

Appendix A: Carbon Balance Terms

The carbon balance equations specific for each tested model are discussed in section 2.3. In this appendix the common terms for both models will be presented.

Maintenance respiration (Re , kg DM m⁻² d⁻¹) is calculated as in Sitch et al. (2003) based on tissue specific C:N ratios, air temperature, tissue biomass and phenology.

Part of the daily net primary production (NPP , kg DM m⁻²), namely $(T \cdot WUE \cdot \rho_v \cdot \omega - Re)$ for the WUE-model and $(LUE \cdot \varepsilon \cdot PAR \cdot FPAR - Re)$ for the LUE-model, is allocated to leaves through the fractional leaf allocation factor φ :

$$\varphi = 1 - \frac{LAI}{LAI_{max}} \quad (A1)$$

where LAI is the simulated leaf area index within vegetated areas and LAI_{max} (m² leaf m⁻² vegetated area) is the maximum LAI supported by the system, considering the plant species and the type of environment.

Leaf area index within vegetated areas is simulated through the specific leaf area factor (SLA , m² leaf kg⁻¹ leaf DM):

$$LAI = B_l \cdot SLA \quad (A2)$$

To obtain ground based leaf area index (LAI_{mod} , m² leaf m⁻² ground) it is necessary to scale LAI by the vegetation fractional cover:

$$LAI_{mod} = LAI \cdot f_t \quad (A3)$$

In addition, to make LAI_{mod} comparable with the LAI obtained from NDVI, average plant water stress of the previous 10 days ($\bar{\zeta}_{10}$) is taken into account as in Williams and Albertson (2005):

$$LAI_{mod}^* = LAI_{mod} \cdot (1 - \bar{\zeta}_{10}) \quad (A4)$$

This is because NDVI is influenced by leaf water content (Dawson *et al.*, 1998) because of changes in chlorophyll content, as discussed in section 2.3. The water stress is obtained as in Porporato *et al.* (2001)

$$\zeta(H_i) = \begin{cases} 0 & \text{for } H_i \geq H_{i,cr} \\ \left(\frac{H_{i,cr} - H_i}{H_{i,cr} - H_{i,lim}} \right)^3 & \text{for } H_{i,lim} < H_i < H_{i,cr} \\ 1 & \text{for } H_i \leq H_{i,lim} \end{cases} \quad (A5)$$

where index i ($=1$ or 2) identifies the shallower or the deeper soil layer.

Vegetation total water stress ζ is calculated as $\zeta(H_1) \cdot r_1 + \zeta(H_2) \cdot (1 - r_1)$.

Appendix B: Hydrological processes

Water balance is performed daily for the two superimposed layers into which the effective root zone is divided: a surficial layer, with thickness d_1 (mm) and water content H_1 (mm H₂O), and a deep layer, with thickness d_2 (mm) and water content H_2 (mm H₂O), similar to Scanlon and Albertson (2003):

$$\frac{dH_1}{dt} = (P - I) - D - E - T_1 \quad (B1)$$

$$\frac{dH_2}{dt} = D - L - T_2 \quad (B2)$$

where t is time (d), P is precipitation, I is leaf interception, D is vertical water flux from the first to the second soil compartment, L is leakage, E is bare soil evaporation, and T is plant transpiration, all with dimensions of mm d^{-1} per unit of ground area. Subscripts 1 and 2 refer to surficial and deep soil layer respectively. The process of bare soil evaporation has access to the soil moisture of the surficial zone, while plants can use water from both zones, in proportion to the root density in each one.

Interception follows:

$$I = \min(P \cdot f_t, I_{\max} \cdot f_t - J) \quad (\text{B3})$$

where I_{\max} is the maximum possible leaf water interception (mm d^{-1}), f_t is the fractional cover and J (mm) is the interception storage, which is subjected to evaporation:

$$\frac{dJ}{dt} = I - \min(ET_o \cdot f_t, J) \quad (\text{B4})$$

Vertical soil water flux (D) and leakage (L) are calculated as “overflows” from the first and the second soil compartments respectively, as in the cascading bucket models: when water thickness of a soil layer exceeds the maximum storage capacity for that zone ($H_{1\max}$, $H_{2\max}$), the excess of water flows to the following soil layer (D , from layer 1 to layer 2) and percolates out of the effective root depth (L , when storage capacity of layer 2 is exceeded). Bare soil evaporation is simulated as:

$$E = ET_o \cdot f_b \cdot \beta_b(H_1) \quad (\text{B5})$$

where $f_b = 1 - f_t$ is the bare soil fraction and β_b is the bare soil water limitation function.

Plant transpiration ($T = T_1 + T_2$) is modelled taking into account the reduction of available energy due to evaporation of intercepted water:

$$T_1 = (ET_o \cdot f_t - \min(ET_o \cdot f_t, J)) \cdot \min(LAI_{mod}, 1) \cdot \beta_t(H_1) \cdot r_1 \quad (B6)$$

$$T_2 = (ET_o \cdot f_t - \min(ET_o \cdot f_t, J)) \cdot \min(LAI_{mod}, 1) \cdot \beta_t(H_2) \cdot (1 - r_1) \quad (B7)$$

where LAI_{mod} is the simulated leaf area index, β_t is the water limitation function for trees and r_1 is the fraction of tree roots in the upper soil layer. Reference evaporation (ET_o , mm d⁻¹) was estimated following the Hargreaves equation as calibrated in the study area by Gavilán et al. (2006):

$$ET_o = 0.0023 \cdot R_a \cdot (Temp + 17.8) \cdot \sqrt{Temp_{max} - Temp_{min}} \quad (B8)$$

where R_a is the water equivalent of the extraterrestrial radiation in mm d⁻¹ (Allen et al., 1998); $Temp$, $Temp_{max}$ and $Temp_{min}$ are the daily mean, maximum and minimum air temperature (C°) where $Temp$ is the average of $Temp_{max}$ and $Temp_{min}$. The soil water limitation functions are

$$\beta_j(H_i) = \begin{cases} 1 & \text{for } H_i \geq H_{i,cr} \\ \left(\frac{H_i - H_{i,lim}}{H_{i,cr} - H_{i,lim}} \right)^m & \text{for } H_{i,lim} < H_i < H_{i,cr} \\ 0 & \text{for } H_i \leq H_{i,lim} \end{cases} \quad (B9)$$

where subscript j (= b or t) indicates bare soil or tree land cover respectively, and it is linked to exponent m (= 1 for bare soil; = 3 for vegetation). Subscript i (= 1 or 2) refers to the soil layer involved. H_{lim} and H_{cr} are the water storages (mm) corresponding respectively to the wilting point and the critical point, below which transpiration is limited (Laio et al., 2001). Water storage values are obtained multiplying soil depth (d_1 and d_2) by soil moisture. The power function proposed by Clapp and Hornberger (1978) is used as soil water retention relationship to obtain soil moisture (θ) at specific soil states:

$$\psi = \psi_{ae} \cdot \left(\frac{n}{\theta} \right)^b \quad (B10)$$

where Ψ (MPa) is the matric potential at the analyzed state, Ψ_{ae} (MPa) is the air entry matric potential, n is porosity, b is an index related to porosity distribution and θ ($\text{m}^3 \text{H}_2\text{O m}^{-3}$ soil) is the volumetric soil moisture. For wilting and critical points, Ψ assumes the values 3 and 0.03 MPa respectively (Laio *et al.*, 2001).

Acknowledgments: The research leading to these results has received funding from the Spanish Ministry of Economy and Competitiveness through the research projects FLOOD-MED (ref. CGL2008-06474-C02-02), SCARCE-CONSOLIDER (ref. CSD2009-00065) and ECO-TETIS (ref. CGL2011-28776-C02-01), and from the European Community's Seventh Framework Programme (FP7 2007-2013) under grant agreement n° 238366. The MODIS data were obtained through the online Data Pool at the NASA Land Processes Distributed Active Archive Center (LP DAAC), USGS/Earth Resources Observation and Science (EROS) Center, Sioux Falls, South Dakota (https://lpdaac.usgs.gov/get_data). The meteorological data were provided by the Spanish National Weather Agency (AEMET). The authors thank Antonio Del Campo García and María González Sanchis at the Universitat Politècnica de València for their support and valuable comments.

References

- Allen RG, Pereira LS, Raes D, Smith M. 1998. Crop evapotranspiration-Guidelines for computing crop water requirements-FAO Irrigation and drainage paper 56. *FAO, Rome* **300**: 6541.
- Anselmi S, Chiesi M, Giannini M, Manes F, Maselli F. 2004. Estimation of Mediterranean forest transpiration and photosynthesis through the use of an ecosystem simulation model driven by remotely sensed data. *Global Ecology and Biogeography* **13**: 371–380. DOI: 10.1111/j.1466-822X.2004.00101.x
- Arora V. 2002. Modeling vegetation as a dynamic component in soilvegetation-atmosphere transfer schemes and hydrological models. *Reviews of Geophysics* **40**: 1006. DOI: 10.1029/2001RG000103

- Awada T, Radoglou K, Fotelli MN, Constantinidou HIA. 2003. Ecophysiology of seedlings of three Mediterranean pine species in contrasting light regimes. *Tree Physiology* **23**: 33–41. DOI: 10.1093/treephys/23.1.33
- Baquedano FJ, Castillo FJ. 2006. Comparative ecophysiological effects of drought on seedlings of the Mediterranean water-saver *Pinus halepensis* and water-spenders *Quercus coccifera* and *Quercus ilex*. *Trees-Structure and Function* **20**: 689–700. DOI: 10.1007/s00468-006-0084-0
- Beven K, Binley A. 1992. The future of distributed models: model calibration and uncertainty prediction. *Hydrological Processes* **6**: 279–298. DOI: 10.1002/hyp.3360060305
- Borghetti M, Cinnirella S, Magnani F, Saracino A. 1998. Impact of long-term drought on xylem embolism and growth in *Pinus halepensis* Mill. *Trees-Structure and Function* **12**: 187–195. DOI: 10.1007/PL00009709
- Calatayud V, Muñoz C, Hernández R, Sanz MJ, Pérez Fortea V, Soldevilla C, Sánchez G. 2000. Seguimiento de daños en acículas de *Pinus halepensis* en localidades de Teruel y Castellón (España). *Ecología* **14**: 129–140.
- Cayrol P, Chehbouni A, Kergoat L, Dedieu G, Mordelet P, Nouvellon Y. 2000. Grassland modeling and monitoring with SPOT-4 VEGETATION instrument during the 1997–1999 SALSA experiment. *Agricultural and Forest Meteorology* **105**: 91–115.
- Ceballos Y, Ruiz de la Torre J. 1979. *Árboles y arbustos de la España peninsular*. ETSI Montes Publications: Madrid.
- Clapp RB, Hornberger GM. 1978. Empirical equations for some soil hydraulic properties. *Water Resources Research* **14**: 601–604.
- Crockford RH, Richardson DP. 1990. Partitioning of rainfall in a eucalypt forest and pine plantation in southeastern Australia: IV The relationship of interception and canopy storage capacity, the interception of these forests, and the effect on interception of thinning the pine plantation. *Hydrological Processes* **4**: 169–188.
- Dawson TP, Curran PJ, Plummer SE. 1998. LIBERTY—modeling the effects of leaf biochemical concentration on reflectance spectra. *Remote Sensing of Environment* **65**: 50–60. DOI: 10.1016/S0034-4257(98)00007-8

- Evrendilek F, Gulbeyaz O. 2008. Deriving vegetation dynamics of natural terrestrial ecosystems from MODIS NDVI/EVI data over Turkey. *Sensors* **8**: 5270–5302. DOI: 10.3390/s8095270
- Gao X, Huete AR, Ni W, Miura T. 2000. Optical–biophysical relationships of vegetation spectra without background contamination. *Remote Sensing of Environment* **74**: 609–620. DOI: 10.1016/S0034-4257(00)00150-4
- García-Plé C, Vanrell P, Morey M. 1995. Litter fall and decomposition in a *Pinus halepensis* forest on Mallorca. *Journal of Vegetation Science* **6**: 17–22. DOI: 10.2307/3236251
- Gavilan P, Lorite IJ, Tornero S, Berengena J. 2006. Regional calibration of Hargreaves equation for estimating reference ET in a semiarid environment. *Agricultural water management* **81**: 257–281. DOI: 10.1016/j.agwat.2005.05.001
- Gigante V, Iacobellis V, Manfreda S, Milella P, Portoghesi I. 2009. Influences of Leaf Area Index estimations on water balance modeling in a Mediterranean semi-arid basin. *Natural Hazards and Earth System Sciences* **9**: 979–991. DOI: 10.5194/nhess-9-979-2009
- Green CF, Hebblethwaite PD, Ison DA. 1985. A quantitative analysis of varietal and moisture status effects on the growth of *Vicia faba* in relation to radiation absorption. *Annals of Applied Biology* **106**: 143–155. DOI: 10.1111/j.1744-7348.1985.tb03104.x
- Hannah DM, Wood PJ, Sadler JP. 2004. Ecohydrology and hydroecology: A ‘new paradigm’? *Hydrological Processes* **18**: 3439–3445. DOI: 10.1002/hyp.5761
- De las Heras J, Moya D, López-Serrano FR, Rubio E. 2013. Carbon sequestration of naturally regenerated Aleppo pine stands in response to early thinning. *New Forests* **44**: 457–470. DOI: DOI 10.1007/s11056-012-9356-2
- Hornberger GM, Spear RC. 1980. Eutrophication in Peel Inlet—I. The problem-defining behavior and a mathematical model for the phosphorus scenario. *Water Research* **14**: 29–42. DOI: 10.1016/0043-1354(80)90039-1

- Huete AR, Justice CO, Van Leeuwen WJD. 1999. MODIS vegetation index (MOD 13). Version 3. Algorithm theoretical basis document. *Greenbelt, MD: NASA, Goddard Space Flight Center*. 120.
- Huete AR, Didan K, Miura T, Rodriguez EP, Gao X, Ferreira LG. 2002. Overview of the radiometric and biophysical performance of the MODIS vegetation indices. *Remote Sensing of Environment* **83**: 195–213. DOI: 10.1016/S0034-4257(02)00096-2
- IPCC. 2007. *Climate Change 2007: Synthesis Report. Contribution of Working Groups I, II and III to the Fourth Assessment Report of the Intergovernmental Panel on Climate Change*. Core Writing Team, Pachauri, R.K and Reisinger, A. (eds.): Geneva, Switzerland.
- Istanbulluoglu E, Wang T, Wedin DA. 2012. Evaluation of ecohydrologic model parsimony at local and regional scales in a semiarid grassland ecosystem. *Ecohydrology* **5**: 121–142. DOI: 10.1002/eco.211
- Jackson RD, Huete AR. 1991. Interpreting vegetation indices. *Preventive Veterinary Medicine* **11**: 185–200. DOI: 10.1016/S0167-5877(05)80004-2
- Jarvis PG, Leverenz JW, others. 1983. Productivity of temperate, deciduous and evergreen forests. *Encyclopedia of Plant Physiology* **12**: 234–280.
- Knorr W, Heimann M. 1995. Impact of drought stress and other factors on seasonal land biosphere CO₂ exchange studied through an atmospheric tracer transport model. *Tellus B* **47**: 471–489. DOI: 10.1034/j.1600-0889.47.issue4.7.x
- Knyazikhin Y, Glassy J, Privette JL, Tian Y, Lotsch A, Zhang Y, Wang Y, Morisette JT, Votava P, Myneni RB, *et al.* 1999. MODIS leaf area index (LAI) and fraction of photosynthetically active radiation absorbed by vegetation (FPAR) product (MOD15) algorithm theoretical basis document. *Theoretical Basis Document, NASA Goddard Space Flight Center, Greenbelt, MD*.
- Kyparissis A, Petropoulou Y, Manetas Y. 1995. Summer survival of leaves in a soft-leaved shrub (*Phlomis fruticosa* L., Labiatae) under Mediterranean field conditions: avoidance of photoinhibitory damage through decreased chlorophyll contents. *Journal of Experimental Botany* **46**: 1825–1831. DOI: 10.1093/jxb/46.12.1825

- Lacaze B, Caselles V, Coll C, Hill J, Hoff C, De Jong S, Mehl W. 1996. *DeMon: Integrated approaches to desertification mapping and monitoring in the mediterranean basin*. Space Applications Inst., Environmental Mapping and Modelling Unit: Italy.
- Laio F, Porporato A, Ridolfi L, Rodriguez-Iturbe I. 2001. Plants in water-controlled ecosystems: active role in hydrologic processes and response to water stress. II. Probabilistic soil moisture dynamics. *Advances in Water Resources* **24**: 707–723. DOI: 10.1016/S0309-1708(01)00005-7
- Li SG, Eugster W, Asanuma J, Kotani A, Davaa G, Oyunbaatar D, Sugita M. 2008. Response of gross ecosystem productivity, light use efficiency, and water use efficiency of Mongolian steppe to seasonal variations in soil moisture. *Journal of Geophysical Research* **113**: G01019. DOI: 10.1029/2006JG000349
- López-Serrano FR, Landete-Castillejos T, Martínez-Millán J, Cerro-Barja A. 2000. LAI estimation of natural pine forest using a non-standard sampling technique. *Agricultural and Forest Meteorology* **101**: 95–111. DOI: 10.1016/S0168-1923(99)00171-9
- Le Maitre DC, Scott DF, Colvin C. 1999. Review of information on interactions between vegetation and groundwater. *Water SA* **25**: 137–152. DOI: 0378-4738
- McCree KJ. 1972. The action spectrum, absorptance and quantum yield of photosynthesis in crop plants. *Agricultural Meteorology* **9**: 191–216. DOI: 10.1016/0002-1571(71)90022-7
- Medici C, Wade AJ, Francés F. 2012. Does increased hydrochemical model complexity decrease robustness? *Journal of Hydrology* **440-441**: 1–13. DOI: 10.1016/j.jhydrol.2012.02.047
- Medlyn BE. 1998. Physiological basis of the light use efficiency model. *Tree Physiology* **18**: 167–176.
- Molina AJ, del Campo AD. 2012. The effects of experimental thinning on throughfall and stemflow: A contribution towards hydrology-oriented silviculture in Aleppo pine plantations. *Forest Ecology and Management* **269**: 206–213. DOI: 10.1016/j.foreco.2011.12.037
- Montaldo N, Rondena R, Albertson JD, Mancini M. 2005. Parsimonious modeling of vegetation dynamics for ecohydrologic studies of water-

- limited ecosystems. *Water Resources Research* **41**: W10416. DOI: 10.1029/2005WR004094
- Monteith JL. 1965. Evaporation and environment. *Symposia of the Society for Experimental Biology* **19**: 205–234.
- Monteith JL. 1972. Solar radiation and productivity in tropical ecosystems. *Journal of Applied Ecology* **9**: 747–766.
- Monteith JL, Moss CJ. 1977. Climate and the efficiency of crop production in Britain [and discussion]. *Philosophical Transactions of the Royal Society B, Biological Sciences* **281**: 277–294. DOI: 10.1098/rstb.1977.0140
- Mu Q, Zhao M, Running SW. 2011. Improvements to a MODIS global terrestrial evapotranspiration algorithm. *Remote Sensing of Environment* **115**: 1781–1800. DOI: 10.1016/j.rse.2011.02.019
- Muñoz C, Pérez V, Cobos P, Hernández R, Sánchez G. 2003. Sanidad forestal. Guía en Imágenes de Plagas, Enfermedades y Otros Agentes Presentes en los Bosques. *Mundi Prensa. Madrid*.
- Myneni R, Hoffman S, Knyazikhin Y, Privette JL, Glassy J, Tian Y, Song X, Zhang Y, Smith GR, Lotsch A, Friedl M, Morisette JT, Votava P, Nemani RR, Running SW. 2002. Global products of vegetation leaf area and fraction absorbed PAR from year one of MODIS data. *Remote Sensing of Environment* **83**: 214-231.
- Myneni R, Knyazikhin Y, Glassy J, Votava P, Shabanov N. 2003. User's Guide: FPAR, LAI (ESDT: MOD15A2) 8-Day Composite NASA MODIS Land Algorithm. Boston University, Boston, MA.
- NASA. 2012. MOD13Q1 version-5. LP DAAC, Sioux Falls, SD.
- Pardos M, Climent J, Gil L, Pardos JA. 2003. Shoot growth components and flowering phenology in grafted *Pinus halepensis* Mill. *Trees-Structure and Function* **17**: 442–450. DOI: 10.1007/s00468-003-0259-x
- Polley HW, Phillips RL, Frank AB, Bradford JA, Sims PL, Morgan JA, Kiniry JR. 2011. Variability in light-use efficiency for gross primary productivity on Great Plains grasslands. *Ecosystems* **14**: 15–27. DOI: 10.1007/s10021-010-9389-3
- Ponce-Campos GE, Moran MS, Huete A, Zhang Y, Bresloff C, Huxman TE, Eamus D, Bosch DD, Buda AR, Gunter SA, et al.. 2013. Ecosystem

- resilience despite large-scale altered hydroclimatic conditions. *Nature* **494**: 349–352. DOI: 10.1038/nature11836
- Porporato A, Laio F, Ridolfi L, Rodriguez-Iturbe I. 2001. Plants in water-controlled ecosystems: active role in hydrologic processes and response to water stress. III. Vegetation water stress. *Advances in Water Resources* **24**: 725–744. DOI: 10.1016/S0309-1708(01)00006-9
- Renard KG, Lane LJ, Simanton JR, Emmerich WE, Stone JJ, Weltz MA, Goodrich DC, Yakowitz DS. 1993. Agricultural impacts in an arid environment: Walnut Gulch studies. *Hydrological Science and Technology* **9**: 145–190.
- Rodriguez-Iturbe I, Porporato A, Laio F, Ridolfi L. 2001. Plants in water-controlled ecosystems: active role in hydrologic processes and response to water stress. I. Scope and general outline. *Advances in Water Resources* **24**: 695–705. DOI: 10.1016/S0309-1708(01)00004-5
- Ruimy A, Kergoat L, Bondeau A, others. 1999. Comparing global models of terrestrial net primary productivity (NPP): analysis of differences in light absorption and light-use efficiency. *Global Change Biology* **5**: 56–64. DOI: 10.1046/j.1365-2486.1999.00007.x
- Running SW, Thornton PE, Nemani RR, Glassy JM. 2000. Global terrestrial gross and net primary productivity from the earth observing system. In: Sala OE, Jackson RB, Mooney HA (Eds.). *Methods in Ecosystem Science*. Springer-Verlag, New York, pp. 44-57
- Running SW, Nemani RR, Heinsch FA, Zhao MS, Reeves M, Hashimoto H. 2004. A continuous satellite-derived measure of global terrestrial primary production. *Bioscience* **54**: 547–560. DOI: 10.1641/0006-3568(2004)054[0547:ACSMOG]2.0.CO;2
- Sabaté S, Gracia CA, Sánchez A. 2002. Likely effects of climate change on growth of *Quercus ilex*, *Pinus halepensis*, *Pinus pinaster*, *Pinus sylvestris* and *Fagus sylvatica* forests in the Mediterranean region. *Forest Ecology and Management* **162**: 23–37. DOI: 10.1016/S0378-1127(02)00048-8
- Scanlon BR, Levitt DG, Reedy RC, Keese KE, Sully MJ. 2005. Ecological controls on water-cycle response to climate variability in deserts. *Proceedings of the National Academy of Sciences* **102**: 6033–6038. DOI: 10.1073/pnas.0408571102

- Scanlon BR, Keese KE, Flint AL, Flint LE, Gaye CB, Edmunds WM, Simmers I. 2006. Global synthesis of groundwater recharge in semiarid and arid regions. *Hydrological Processes* **20**: 3335–3370. DOI: 10.1002/hyp.6335
- Scanlon TM, Albertson JD. 2003. Inferred controls on tree/grass composition in a savanna ecosystem: Combining 16-year normalized difference vegetation index data with a dynamic soil moisture model. *Water Resources Research* **39**: 1224. DOI: 10.1029/2002WR001881
- Sellers PJ, Tucker CJ, Collatz GJ, Los SO, Justice CO, Dazlich DA, Randall DA. 1996. A revised land surface parameterization (SiB2) for atmospheric GCMs. Part II: The generation of global fields of terrestrial biophysical parameters from satellite data. *Journal of Climate* **9**: 706–737. DOI: 10.1175/1520-0442(1996)009<0706:ARLSPF>2.0.CO;2
- Sitch S, Smith B, Prentice IC, Arneth A, Bondeau A, Cramer W, Kaplan JO, Levis S, Lucht W, Sykes MT, *et al.* 2003. Evaluation of ecosystem dynamics, plant geography and terrestrial carbon cycling in the LPJ dynamic global vegetation model. *Global Change Biology* **9**: 161–185. DOI: 10.1046/j.1365-2486.2003.00569.x
- Sprintsin M, Karnieli A, Berliner P, Rotenberg E, Yakir D, Cohen S. 2007. The effect of spatial resolution on the accuracy of leaf area index estimation for a forest planted in the desert transition zone. *Remote Sensing of Environment* **109**: 416–428. DOI: 10.1016/j.rse.2007.01.020
- Sprintsin M, Karnieli A, Berliner P, Rotenberg E, Yakir D, Cohen S. 2009. Evaluating the performance of the MODIS Leaf Area Index (LAI) product over a Mediterranean dryland planted forest. *International Journal of Remote Sensing* **30**: 5061–5069. DOI: 10.1080/01431160903032885
- Teuling AJ, Troch PA. 2005. Improved understanding of soil moisture variability dynamics. *Geophysical Research Letters* **32**: L05404. DOI: 10.1029/2004GL021935
- Tucker CJ. 1979. Red and photographic infrared linear combinations for monitoring vegetation. *Remote Sensing of Environment* **8**: 127–150. DOI: 10.1016/0034-4257(79)90013-0
- Vicente-Serrano SM, Lasanta T, Gracia C. 2010. Aridification determines changes in forest growth in *Pinus halepensis* forests under semiarid

- Mediterranean climate conditions. *Agricultural and Forest Meteorology* **150**: 614–628. DOI: 10.1016/j.agrformet.2010.02.002
- Wade AJ, Hornberger GM, Whitehead PG, Jarvie HP, Flynn N. 2001. On modeling the mechanisms that control in-stream phosphorus, macrophyte, and epiphyte dynamics: An assessment of a new model using general sensitivity analysis. *Water Resources Research* **37**: 2777–2792. DOI: 10.1029/2000WR000115
- Weinstein A. 1989. Geographic variation and phenology of *Pinus halepensis*, *P. brutia* and *P. eldarica* in Israel. *Forest Ecology and Management* **27**: 99–108. DOI: 10.1016/0378-1127(89)90032-7
- Williams CA, Albertson JD. 2005. Contrasting short-and long-timescale effects of vegetation dynamics on water and carbon fluxes in water-limited ecosystems. *Water Resources Research* **41**: W06005. DOI: 10.1029/2004WR003750
- Yuan W, Liu S, Zhou G, Zhou G, Tieszen LL, Baldocchi D, Bernhofer C, Gholz H, Goldstein AH, Goulden ML, *et al.* 2007. Deriving a light use efficiency model from eddy covariance flux data for predicting daily gross primary production across biomes. *Agricultural and Forest Meteorology* **143**: 189–207. DOI: 10.1016/j.agrformet.2006.12.001
- Zalewski M, Janauer GA, Jolankai G. 1997. *Ecohydrology: a new paradigm for the sustainable use of aquatic resources*. UNESCO IHP Technical Document in Hydrology No. 7.; IHP - V Projects 2.3/2.4: UNESCO Paris.